ELSEVIER

Journal of Hazardous Materials 44 (1995) 111–125

JOURNAL OF HAZARDOUS MATERIALS

Drift-flux correlation disengagement models: Part I – Theory: Analytic and numeric integration details

C.M. Sheppard[a,*], S.D. Morris[b]

[a] *Chemical Engineering Department, Louisiana Tech University, P.O. Box 10348 TS, Ruston, LA 71272, USA*

[b] *Safety Technology Institute, Process Engineering Division, TP250 Joint Research Centre, Ispra Commission of the European Communities, 21020 Ispra (VA), Italy*

Received 21 September 1994; accepted 7 April 1995

Abstract

In the design of pressure relief systems for vessels containing liquid, the phase of the flow through the vent line is very important. Mounting the line on the top of the vessel does not necessarily guarantee all vapor flow. One must calculate whether vapor bubbles formed in the liquid will disengage before they reach the vent entrance.

Disengagement can be predicted via an axial void fraction profile that is calculated based upon volumetric gas production. It is assumed that the liquid phase is continuous and that pseudo-steady state is reached. The disengagement model is based on a constant energy generation per unit mass of liquid. For non-foaming systems, one of two drift-flux correlations can be chosen on the basis of viscosity. The churn-turbulent drift-flux correlation is for low-viscosity systems, and the DIERS' viscous-bubbly drift-flux correlation is for high-viscosity system [1, 2]. This model reduces to a single ordinary differential equation (ode). Analytic integration results for this model are possible for constant cross-sectional area vessels (e.g., vertical cylinder) and non-unity distribution parameters *Co* [3–5].

If this calculation shows the bubbles do not disengage, either a partial differential equation model must be solved or the coupling equation must be used. The coupling equation uses the maximum void fraction (calculated from the ode) and ties together the vessel and vent models.

The ode solutions relate the local and average void fractions to the dimensionless superficial vapor velocity. For the churn-turbulent drift-flux correlation, explicit relationships are presented for the first time. They validate the earlier approximation of Fauske et al. [6] (see also Ref. [3]). For the DIERS' viscous-bubbly drift-flux correlation, implicit relationships are presented for the first time in the open literature. The earlier approximation of Fauske et al. [6] (see also Ref. [7]) fit the data, but is different than these integration results. Further work is in progress to refit the data [8] and to clarify the best model to use.

For non-constant cross-sectional area vessels (e.g., horizontal cylinders and spheres), the analytic integration is difficult, but numeric results have been presented [3, 7]. The details of the numeric integration are presented and discussed here. As the cross-sectional area converges

* Corresponding author.

SSDI 0304-3894(95)00051-8

(toward the top of the vessel), the vapor concentration (i.e., the void fraction) and velocity increase. The maximum local void fraction occurs at the top of the vessel. Numerical difficulties are encountered as a result of the cross-sectional area going to zero at the bottom and top of the vessel. The pseudo-steady-state model imposes void fractions of minimum and maximum at these extremes (i.e., 0 and 1/Co).

Keywords: Two-phase flow; Venting; Disengagement; Void fraction; DIERS; Drift-flux correlations; Churn-turbulent; DIERS' viscous bubbly

1. Introduction

The phase of the vent flow is important for emergency relief system design. If bubbles form and the vessel contents swell to the top, two-phase vent flow will occur. The sonic velocity for two-phase flow is a function of void fraction and is typically more than an order of magnitude lower than either liquid or vapor flow. Thus, a larger vent is required. Therefore, predicting the void fraction of the two-phase flow and the point of onset and of disengagement (i.e., cessation of two-phase flow) is crucial for proper pressure relief device design.

Drift-flux correlations are correlations from experimental data of two-phase flow in pipes which relate the relative speed of the vapor to the void fraction of the mixture. These drift-flux correlations are used to describe the movement occurring in the vessel. Earlier work indicated that for non-foaming systems one of two drift-flux correlations can be chosen on the basis of viscosity [1]. They are the churn turbulent and a modified bubbly (i.e., DIERS viscous-bubbly [5]). The churn-turbulent drift-flux correlation is recommended for low-viscosity systems ($\mu < 100$ cP) and the DIERS viscous-bubbly drift-flux correlation for high-viscosity systems [1]. The liquid phase is assumed to be continuous. Liquid entrainment (two-phase flow with the gas phase continuous) is not considered (for information on liquid entrainment, see Refs. [9, 10]).

This paper details the assumptions and simplifications to derive and solve the ordinary differential equation describing disengagement. The work presented in this paper is independent of drift-flux correlation chosen. It is also relevant when two-phase flow does occur. In that case, either the resulting partial differential equations must be solved or the coupling equation can be used to tie together a pseudo-steady-state vessel model with the vent line model. The coupling equation uses a maximum void fraction value calculated from the disengagement model discussed below (see Ref. [9] for a further discussion of this topic). For more background information see Refs. [1, 2, 6].

2. Discussion

Five key model elements are reviewed, including the pseudo-steady-state assumption and the use of drift-flux correlations to predict disengagement. Next, the analyti-

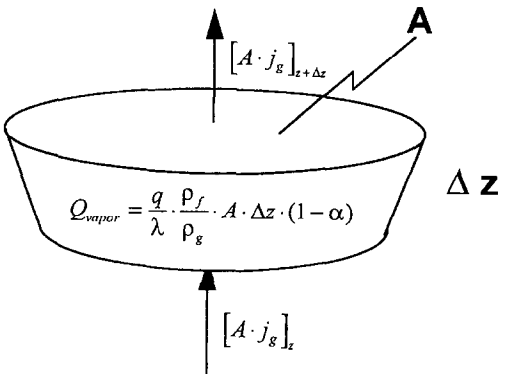

Fig. 1. Differential slice for combined vapor material balance or energy balance.

cal integration results for the local void fraction (α or α_{max} at the top of the vessel) and average void fraction ($\bar{\alpha}$) in constant cross-sectional area vessels (e.g., vertical cylinders) are presented. These results are compared with the DIERS approximation. Following this, the extension to non-constant cross-sectional area vessels via numeric integration is described.

2.1. Disengagement model reviewed

The model is derived for a differential slice as shown in Fig. 1. There are five key elements to this model. The first four are foundational assumptions. The fifth is the boundary conditions. These elements are as follows:

1. vapor generation (e.g., energy input) is proportional to the liquid mass;
2. a distribution parameter can be used to adjust the drift-flux correlation (originally the distribution parameter was used to account for radial gradients in small diameter pipes);
3. pseudo-steady-state conditions occur (i.e., large volumetric vapor production makes a small difference in the liquid volume and thus the liquid velocity ≈ 0);
4. an appropriate drift-flux correlation describes the system behavior;
5. the boundary conditions are such that both the local and average void fractions approach zero at the bottom of the vessel.

The implications of and associated equations for each of the four assumptions are discussed below, as are the average void fraction definition and boundary conditions.

2.1.1. Vapor generation

Vapor generation (e.g., by energy input) is assumed to be proportional to liquid mass. That is, for a differential slice of thickness Δz, the following expressions arise:

$$\textit{Mass of liquid:} \quad M_{\text{liquid}} = \rho_f A \Delta z (1 - \alpha), \tag{1}$$

$$\textit{Energy input:} \quad \text{Energy}_{\text{input}} = q \rho_f A \Delta z (1 - \alpha), \tag{2}$$

$$\textit{Mass of vapor:} \qquad W_{\text{vapor}} = \frac{q}{\lambda}\rho_f A \Delta z (1-\alpha), \tag{3}$$

$$\textit{Volume of vapor:} \qquad Q_{\text{vapor}} = \frac{q}{\lambda}\frac{\rho_f}{\rho_g} A \Delta z (1-\alpha). \tag{4}$$

Note that the area A can be a function of height z.

2.1.2. Distribution parameter

Zuber and Findley [11] introduced a distribution parameter to account for radial gradients without integrating radially. It was defined as the ratio of the average of the product of flux times void fraction to the product of average of flux and of void fraction (i.e., $Co = \langle \alpha j \rangle / \langle \alpha \rangle \langle j \rangle$). According to Wallis [12], *Co*... usually lies between 1.0 and 1.5 with a most probable value of about 1.2". As discussed by Zuber and Findley [11], a distribution parameter of 1.5 indicates a very large radial gradient.

However, large diameter vessels are common in the chemical process industry. Therefore, a very small radial gradient is expected. DIERS [2] recommends values of 1.5 for the churn-turbulent case and 1.2 for the DIERS' viscous-bubbly case. Since this value is much larger than would be expected in a process vessel, Fisher [13] suggests that the churn-turbulent distribution parameter value is high and may be viewed as a fitting parameter. The most appropriate DIERS' viscous-bubbly distribution parameter is currently under discussion. Sheppard [14] suggests 1.5 *may* be better, but a more definitive recommendation should be available in late 1995 [8].

2.1.3. Pseudo-steady-state conditions

Vapor bubbles are expected to form in the bulk, and to rise up, moving faster than the liquid, swelling the vessel contents. Assuming pseudo-steady state, the interface is below the vent, the bubbles will break though the interface, and all vapor venting will occur. The interface will slowly fall, as material leaves the system. Since a large increase in vapor volume makes only a small decrease in the liquid volume, the liquid velocity is small, and can be assumed to be zero (i.e., $j_f \approx 0$).

For the differential slice shown in Fig. 1, the definition for drift flux is

$$j_{gf} \equiv (1 - Co\alpha) j_g - Co\alpha j_f \tag{5}$$

The equation simplifies for a distribution parameter Co of unity.

Using the pseudo-steady-state assumption (i.e., $j_f = 0$) the general drift-flux equation becomes

$$j_g \approx \frac{j_{gf}}{(1 - Co\alpha)}. \tag{6}$$

Using the other assumptions, for the differential slice, the material balance becomes a differential vapor balance, or, equivalently, an energy balance as follows:

$$\begin{matrix}\text{Vapor} \\ \text{in}\end{matrix} + \begin{matrix}\text{Vapor} \\ \text{Generation}\end{matrix} = \begin{matrix}\text{Vapor} \\ \text{out}\end{matrix} + \begin{matrix}\text{rate of Vapor} \\ \text{Accumulation}\end{matrix} \tag{7}$$

$$Aj_g|_z + \frac{q}{\lambda}\frac{\rho_f}{\rho_g} A\,\Delta z(1-\alpha) = Aj_g|_{z+\Delta z} + 0, \tag{8}$$

$$\frac{Aj_g|_{z+\Delta z} - Aj_g|_z}{\Delta z} = \frac{q}{\lambda}\frac{\rho_f}{\rho_g} A(1-\alpha), \tag{9}$$

$$\frac{d}{dz}(j_g A) = \frac{q}{\lambda}\frac{\rho_f}{\rho_g} A(1-\alpha). \tag{10}$$

This expression models the disengagement process; the model is simplified below by the introduction of definitions and completed by including a drift-flux correlation.

The dimensionless superficial vapor velocity ψ is by definition the ratio of superficial vapor velocity $j_{g\infty}$ to bubble rise velocity U_∞. The superficial vapor velocity is the volume of gas produced in the vessel divided by the cross-sectional area of the vessel. The bubble rise velocity is the velocity at which a single bubble rises in an infinite medium of the liquid; it is used in the drift-flux correlation. To simplify the equation, this definition of ψ [6] or the modified dimensionless superficial vapor velocity Ξ can be used. These velocities are defined as follows:

$$\psi = \frac{j_{g\infty}}{U_\infty} = \frac{\rho_f}{\rho_g}\frac{q}{\lambda}\frac{H(1-\bar{\alpha})}{U_\infty}, \tag{11}$$

$$\Xi \equiv \frac{j_{g\infty}}{U_\infty(1-\bar{\alpha})} = \frac{\rho_f}{\rho_g}\frac{q}{\lambda}\frac{H}{U_\infty}. \tag{12}$$

This first definition [6] is based on the volumetric flow of gas coming off the top of an open, constant cross-sectional area vessel. For a non-constant cross-sectional area vessel, the meaning of the dimensionless superficial vapor velocity ψ is not clear. It can be viewed as an equivalent dimensionless superficial vapor velocity for a vertical cylinder. Or, as discussed in Part II [16], the velocity can be calculated based on an average cross-sectional area. Details on the modified dimensionless superficial vapor velocity are given in Ref. [15].

In the derivation below, both dimensionless superficial vapor velocity definitions are used, the first since it is the more widely used and the second because the results are simpler. Using these definitions, the vapor generation rate becomes

$$\frac{q}{\lambda}\frac{\rho_f}{\rho_g} = \Xi\frac{U_\infty}{H} = \frac{\psi}{(1-\alpha)}\frac{U_\infty}{H}. \tag{13}$$

Substituting this result into Eq. (12), gives

$$\frac{d}{dz}(j_g A) = \frac{\Xi U_\infty}{H} A(1-\alpha) = \frac{\psi U_\infty}{H(1-\bar{\alpha})} A(1-\alpha). \tag{14}$$

Defining a dimensionless height (i.e., $z^* = z/H$) gives

$$\frac{d}{dz^*}\left(\frac{j_g}{U_\infty} A\right) = \Xi A(1-\alpha) = \frac{\psi}{(1-\bar{\alpha})} A(1-\alpha). \tag{15}$$

Note that some researchers define dimensionless height in terms of initial liquid height H_0, e.g., Ref. [5]; this definition is not used here.

For constant cross-sectional area vessels this reduces to

$$\frac{\mathrm{d}}{\mathrm{d}z^*}\left(\frac{j_g}{U_\infty}\right) = \Xi(1-\alpha) = \frac{\psi}{(1-\bar{\alpha})}(1-\alpha). \tag{16}$$

Differentiating with respect to α, gives

$$\frac{\mathrm{d}}{\mathrm{d}\alpha}\left(\frac{j_g}{U_\infty}\right)\frac{\mathrm{d}\alpha}{\mathrm{d}z^*} = \Xi(1-\alpha) = \frac{\psi}{(1-\bar{\alpha})}(1-\alpha). \tag{17}$$

2.1.4. Drift-flux correlation

The drift flux is the relative flux or speed of the light phase to the heavy phase (e.g., the vapor flux minus the liquid flux). Experimental data on two-phase flow in small diameter pipes have been measured and exhibit distinct flow regimes. This flux data have been successfully correlated with void fraction for the observed flow regimes. Thus, these correlations are useful for predicting the flow when the expected flow regime has been identified. They are used in Eq. (6) and are differentiated with respect to z for use in Eq. (15) or (17). The results for the two drift-flux correlations of interest follow.

The churn-turbulent drift-flux correlation has the form

$$j_{gf} = U_\infty \alpha, \tag{18}$$

and, using Eq. (6), the relationship between drift flux and vapor volumetric flux, gives

$$\frac{j_g}{U_\infty} = \frac{\alpha}{(1 - Co\alpha)}. \tag{19}$$

Differentiating gives

$$\frac{\mathrm{d}}{\mathrm{d}\alpha}\left(\frac{j_g}{U_\infty}\right) = (1 - Co\alpha)^{-2} \tag{20}$$

as is needed for Eq. (15) or (17).

Similarly, the DIERS' viscous-bubbly drift-flux correlation is a modification of the bubbly drift-flux correlation of Wallis [12]. According to Grolmes and Fisher [5], the term in the denominator was added to 'correlate the departure of viscous material hold-up data from both simple bubble and churn-turbulent relations'. The drift-flux correlation and vapor volumetric flux equations have the following forms for viscous-bubbly flow:

$$j_{gf} = \frac{U_\infty \alpha(1-\alpha)^2}{(1-\alpha^3)}, \tag{21}$$

$$j_g = \frac{U_\infty \alpha(1-\alpha)^2}{(1-\alpha^3)(1 - Co\alpha)}. \tag{22}$$

Differeintiating gives

$$\frac{\mathrm{d}}{\mathrm{d}\alpha}\left(\frac{j_g}{U_\infty}\right) = \frac{-(Co\alpha^4 - 2Co\alpha^3 - 2(Co-1)\alpha^2 + 2\alpha - 1)}{[(\alpha^2+\alpha+1)(1-Co\alpha)]^2} \tag{23}$$

as is needed for Eq. (15) or (17).

2.1.5. Boundary conditions

There are two boundary conditions for the pseudo-steady-state model. At the bottom of the vessel, the local and average void fractions are assumed to approach zero (i.e., $\alpha = 0$ at $z = 0$). To avoid numeric problems, very small void fraction values are used at the bottom of the vessel for the numeric integration (e.g., 10^{-4}). At the top of the vessel, the void fraction reaches its maximum value. Thus, $\alpha|_{top} \equiv \alpha_{max}$ or $\alpha = \alpha_{max}$ at $z = H$ or $z^* = 1$.

For horizontal cylinders, and spheres, the cross-sectional area approaches zero at the top and bottom of the vessel so that the numeric integration fails at these locations. Again we need only start the integration at a very small height (e.g., $z = 10^{-6}$) and end the integration very close to the total height (e.g., $z = 0.999H$). The maximum void fraction occurs at the top of the vessel and will approach the asymptote of $1/Co$ [9].

2.2. Analytic results for constant cross-sectional area vessels

Finally, one can combine the appropriate differentiated drift-flux relationship above with Eq. (17). This single differential equation is integrated to find a relationship between the local void fraction and the dimensionless superficial vapor velocity. Then using the definition of the average void fraction one integrates again to find a relationship between the average void fraction and the dimensionless superficial vapor velocity. This integration process is illustrated below for constant cross-sectional area vessels for the churn-turbulent and DIERS' viscous-bubbly drift-flux correlation. Closed-form solutions are found for both cases.

2.2.1. Churn-turbulent drift-flux correlation

An implicit relationship between dimensionless superficial vapor velocity, average and local void fraction has been presented before [15, 17]. An explicit relationship between average and local void fraction and the dimensionless superficial vapor velocity is presented here.

Substituting Eq. (20) into Eq. (17) gives

$$(1-\alpha)^{-1}(1-Co\alpha)^{-2}\frac{\mathrm{d}\alpha}{\mathrm{d}z^*} = \frac{\psi}{(1-\bar{\alpha})} = \Xi. \tag{24}$$

This is integrated using partial fractions as illustrated below:

$$\Xi z = \frac{\psi}{(1-\bar{\alpha})}z = \int_0^{\alpha}(1-\alpha)^{-1}(1-Co\alpha)^{-2}\,\mathrm{d}\alpha$$

$$= \int_0^{\alpha} \frac{A}{(1-\alpha)} + \frac{B}{1-Co\alpha} + \frac{C}{(1-Co\alpha)^2}\,d\alpha$$

$$= (1-Co)^{-2} \int_0^{\alpha} \frac{1}{(1-\alpha)} + \frac{-Co}{1-Co\alpha} + \frac{Co(Co-1)}{(1-Co\alpha)^2}\,d\alpha$$

$$= (1-Co)^{-2}\left[-\ln(1-\alpha) + \ln(1-Co\alpha) + \frac{Co-1}{1-Co\alpha} \right]_0^{\alpha} \tag{25}$$

so

$$\frac{\psi}{(1-\bar{\alpha})} z^* = \Xi z^* = (Co-1)^{-2}\left[\ln\left\{ \frac{1-Co\alpha}{1-\alpha} \right\} + Co(Co-1) + \frac{\alpha}{(1-Co\alpha)} \right]. \tag{26}$$

This is an implicit relationship between local void fraction and dimensionless superficial vapor velocity (it is explicit in z, but we desire it to be explicit in α).

The definition of the average void fraction is as follows:

$$\bar{\alpha} \equiv \frac{\int_{z^*=0,\alpha=0}^{z^*,\alpha} A\alpha\,dz^*}{\int_{z^*=0}^{z^*} A\,dz^*}. \tag{27}$$

For the constant cross-sectional area case this can be simplified to

$$\bar{\alpha}|_{A=\text{constant}} = \frac{1}{z^*} \int_{z^*=0,\alpha=0}^{z^*,\alpha} \alpha\,dz^*. \tag{28}$$

From the differential material balance, Eq. (24), one obtains

$$dz^* = \Xi^{-1}(1-\alpha)^{-1}(1-Co\alpha)^{-2}\,d\alpha, \tag{29}$$

and substituting this into Eq. (28), the following integration can be performed:

$$\bar{\alpha}|_{A=\text{constant}} = \frac{1}{z^*} \int_{z^*=0,\alpha=0}^{z^*} \alpha\Xi^{-1}(1-\alpha)^{-1}(1-Co\alpha)^{-2}\,d\alpha$$

$$= \frac{1}{z^*\Xi} \int_0^{\alpha} \alpha(1-\alpha)^{-1}(1-Co\alpha)^{-2}\,d\alpha$$

$$= \frac{1}{z^*\Xi} \int_0^{\alpha} \frac{A'}{(1-\alpha)} + \frac{B'}{1-Co\alpha} + \frac{C'}{(1-Co\alpha)^2}\,d\alpha$$

$$= \frac{1}{z^*\Xi}(1-Co)^{-2} \int_0^{\alpha} \frac{1}{(1-\alpha)} + \frac{-Co}{1-Co\alpha} + \frac{(Co-1)}{(1-Co\alpha)^2}\,d\alpha$$

$$= \frac{1}{z^*\Xi}(1-Co)^{-2}\left[-\ln(1-\alpha) + \ln(1-Co\alpha) + \frac{(Co-1)/Co}{1-Co\alpha} \right]_0^{\alpha}. \tag{30}$$

So this second integration leads to the average void fraction relationship:

$$\bar{\alpha}\frac{\psi}{(1-\bar{\alpha})}z^* = \bar{\alpha}\Xi z^* = (Co-1)^{-2}\left[\ln\left\{\frac{1-Co\alpha}{1-\alpha}\right\} + (Co-1)\frac{\alpha}{(1-Co\alpha)}\right]. \quad (31)$$

This is an implicit relationship between average void fraction and dimensionless superficial vapor velocity.

One can subtract Eq. (31) from (26) to obtain the following:

$$\frac{\psi}{(1-\bar{\alpha})}z^*(1-\bar{\alpha}) = \frac{\alpha}{(1-Co\alpha)} \quad (32)$$

$$\psi z^* = \frac{\alpha}{(1-Co\alpha)} = \left[\frac{1}{\alpha} - Co\right]^{-1}. \quad (33)$$

or

$$\alpha = \left[\frac{1}{(\psi z^*)} + Co\right]^{-1}. \quad (34)$$

At the top of the vessel the void fraction is defined as α_{max} (i.e., $\alpha = \alpha_{max}$ at $z^* = 1$)

$$\alpha_{max} = \left[\frac{1}{\psi} + Co\right]^{-1} = \frac{\psi}{1+Co\psi}. \quad (35)$$

Each α_{max} term in Eq. (26) can be formulated in terms of ψ as follows:

$$\frac{1-Co\alpha_{max}}{1-\alpha_{max}} = \frac{1/\alpha_{max} - Co}{1/\alpha_{max} - 1} = \frac{1/\psi + Co - Co}{1/\psi + Co - 1}$$

$$= [1 + (Co-1)\psi]^{-1}, \quad (36)$$

$$\frac{\alpha_{max}}{1-Co\alpha_{max}} = \frac{1}{1/\alpha_{max} - Co} = \psi. \quad (37)$$

Using these results in Eq. (26), one obtains

$$\frac{\psi}{(1-\bar{\alpha})} = \Xi = (Co-1)^{-2}[-\ln[1+(Co-1)\psi] + Co(Co-1)\psi], \quad (38)$$

or

$$\bar{\alpha} = 1 + \psi(1-Co)^2\{\ln[1+(Co-1)\psi] - Co(Co-1)\psi\}^{-1}. \quad (39)$$

So explicit analytic equations for the local and average void fractions, as a function of ψ, have been derived (i.e., Eqs. (37) and (39)). Sheppard [15] found reasonable agreement between the analytical $\bar{\alpha}$ results and the approximation suggested by DIERS [6] which follows (see Fig. 2):

$$\bar{\alpha} \approx \frac{\psi}{2+Co\psi}. \quad (40)$$

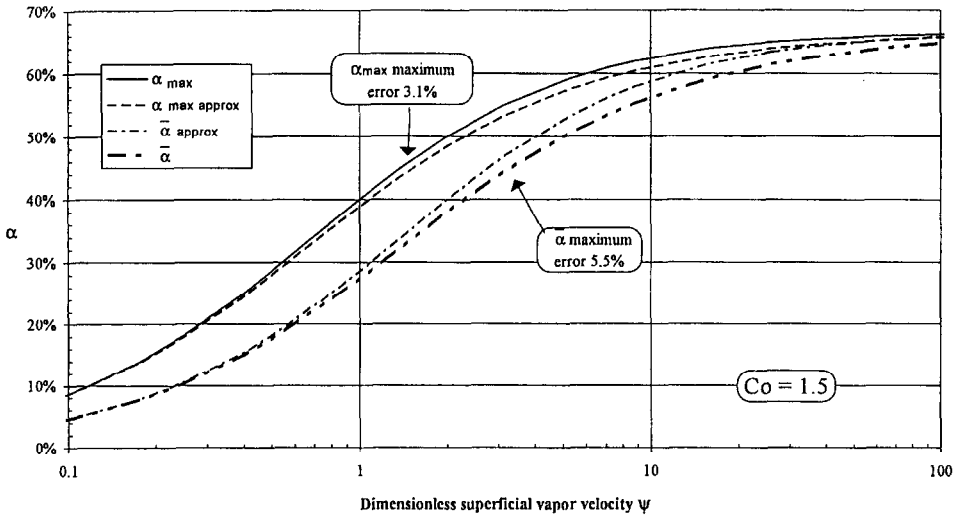

Fig. 2. Vertical cylinders local and average void fraction analytic integration results and DIERS approximations compared for the churn-turbulent drift-flux correlation.

Fig. 2 also shows a comparison between the analytical α_{max} results and the approximation suggested by DIERS [6], or

$$\alpha_{max} \approx \frac{2\bar{\alpha}}{1 + Co\bar{\alpha}}. \tag{41}$$

As Fig. 2 shows the approximations are reasonable. The maximum void fraction is underpredicted by, at most, 3.1% (with this maximum deviation occurring around a ψ value of 2). The average void fraction is overpredicted by, at most, 5.5% (with this maximum deviation occurring at a ψ value between 3 and 4). But since exact explicit equations are now known, there is a little reason to use the approximations.

2.2.2. *DIERS' viscous-bubbly drift-flux correlation*

For the DIERS' viscous-bubbly case, an analytic expression for the vertical cylinder case is included. This expression was reported by Morris [4] and confirmed by Grolmes [5].

For the constant cross-sectional area case (e.g., a vertical cylinder) the derivative of the cross-sectional area with respect to height is zero, which simplifies the vapor material balance (Eq. (19)). Then, the DIERS' viscous-bubbly drift-flux correlation and its derivative can be used along with the average void fraction definition. After some algebra and two integrations, the following expressions are obtained [4]:

$$\psi = \frac{\alpha_{max}(1 - \alpha_{max})^2}{(1 - \alpha_{max}^3)(1 - Co\alpha_{max})}, \tag{42}$$

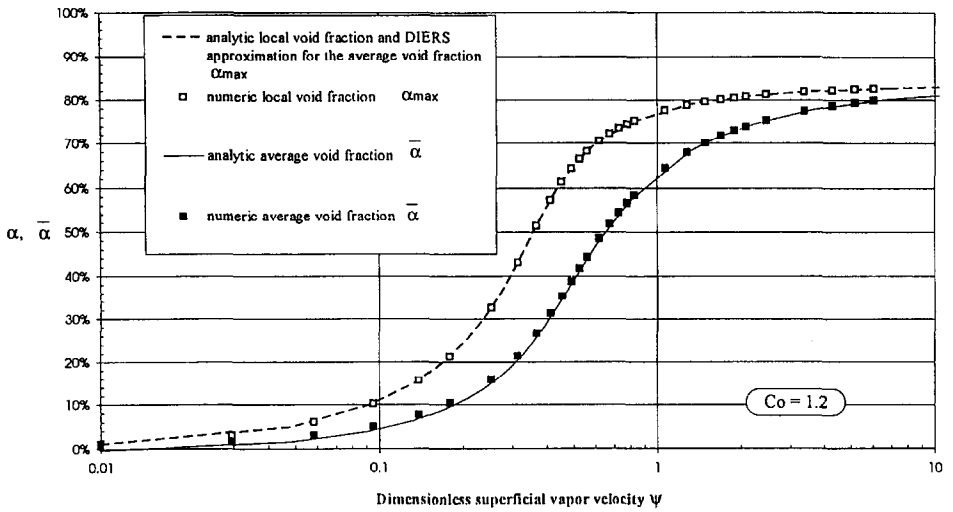

Fig. 3. Analytic local and average void fraction integration results and DIERS approximations compared for the DIERS' viscous-bubbly drift-flux correlation.

$$\bar{\alpha} = \frac{\alpha_{max} x + y}{x + y} = \frac{\alpha_{max} + y/x}{1 + y/x}, \tag{43}$$

where

$$x = \frac{\alpha_{max}}{(1 + \alpha_{max} + \alpha_{max}^2)(1 - Co\alpha_{max})} = \frac{\alpha_{max}(1 - \alpha_{max})}{(1 - \alpha_{max}^3)(1 - Co\alpha_{max})}, \tag{44}$$

$$y = \left[\frac{Co - 1}{6(Co^2 + Co + 1)}\right] \ln\left[\frac{1 + \alpha_{max} + \alpha_{max}^2}{(1 - \alpha_{max})^2}\right] - \left[\frac{Co}{Co^3 - 1}\right] \ln\left[\frac{1 - \alpha_{max}}{1 - Co\alpha_{max}}\right] + \left[\frac{Co + 1}{\sqrt{3}(Co^2 + Co + 1)}\right] \tan^{-1}\left[\frac{\sqrt{3}\alpha_{max}}{2 + \alpha_{max}}\right]. \tag{45}$$

This is an implicit relationship between the maximum void fraction, average void fraction, and the dimensionless superficial vapor velocity. It is readily evaluated for a given value of α_{max} giving the corresponding values of ψ and $\bar{\alpha}$. Morris [4] also provides a correlation between the local and average void fraction at the top of the vessel (i.e., α_{max} and $\bar{\alpha}$).

Morris [4] and Sheppard [7] also found poor agreement (see Fig. 3) between the numeric $\bar{\alpha}$ results to the approximation suggested by DIERS [6], which follows

$$\psi \approx \frac{\bar{\alpha}(1 - \bar{\alpha})^2}{(1 - \bar{\alpha}^3)(1 - Co\bar{\alpha})}. \tag{46}$$

In light of the above analytic integration results, this result is not surprising. The approximation suggested for the average void fraction is the exact relationship for the

maximum or local void fraction. Since the local void fraction is always greater than the average, the agreement is poor. Even though the approximation is not reasonable, it was reported to agree with the data [1, 6]. The exact implicit equations are now known. However, it is not clear which equations should now be used. Grolmes and Fisher [5] discuss this briefly, and still recommend that the maximum void fraction be set equal to the average void fraction (i.e., $\alpha_{max} = \bar{\alpha}$). Further discussion is anticipated in Ref. [8] and with all the available data being included in the comparison (e.g., the Joint Research Centre multiphase multicomponent facility data [18, 19]).

2.3. *Non-constant cross-sectional area vessel case and numeric integration details*

To develop average void fraction equations for horizontal cylinders and spheres, the first step is to expand differential vapor balance using the product rule as follows:

$$\frac{\mathrm{d}}{\mathrm{d}z^*}\left(\frac{j_g}{U_\infty}A\right) = \Xi A(1-\alpha) = \frac{\psi}{(1-\bar{\alpha})}A(1-\alpha), \tag{15}$$

$$\frac{\mathrm{d}}{\mathrm{d}z^*}\left(\frac{j_g}{U_\infty}A\right) = A\frac{\mathrm{d}}{\mathrm{d}\alpha}\left(\frac{j_g}{U_\infty}\right)\frac{\mathrm{d}\alpha}{\mathrm{d}z^*} + \frac{j_g}{U_\infty}\frac{\mathrm{d}A}{\mathrm{d}z^*} \tag{47}$$

or rearranging

$$\frac{\mathrm{d}\alpha}{\mathrm{d}z^*} = \left[\Xi(1-\alpha) - \frac{1}{A}\left(\frac{j_g}{U_\infty}\right)\frac{\mathrm{d}A}{\mathrm{d}z}\right] \Big/ \frac{\mathrm{d}}{\mathrm{d}\alpha}\left(\frac{j_g}{U_\infty}\right). \tag{48}$$

The relationships for cross-sectional area with height for the horizontal cylinder and sphere are as follows:

$$A_{\text{horizontal cylinder}} = 2L\sqrt{2Rz - z^2}, \qquad A_{\text{sphere}} = \pi(2Rz - z^2). \tag{49a, b}$$

Differentiating with respect to z:

$$\frac{\mathrm{d}A_{\text{horizontal cylinder}}}{\mathrm{d}z} = \frac{2L(R-z)}{\sqrt{2Rz - z^2}}, \qquad \frac{\mathrm{d}A_{\text{sphere}}}{\mathrm{d}z} = 2\pi(R-z). \tag{50a, b}$$

The average void fraction equation can be split, based upon the integration required in the numerator and denominator. Then one obtains the following two integrations, respectively:

$$V_{\text{bubbles}} = \int_{z=0,\alpha=0}^{z^*,\alpha} A\alpha\,\mathrm{d}z^*, \qquad V_{\text{vessel}} = \int_{z^*=0}^{z^*} A\,\mathrm{d}z^*. \tag{51a, b}$$

Differentiating

$$\frac{\mathrm{d}V_{\text{bubbles}}}{\mathrm{d}z} = A\alpha, \tag{52}$$

$$\frac{\mathrm{d}V_{\text{vessel}}}{\mathrm{d}z} = A. \tag{53}$$

The definitions of the average void fraction and its relationship, in terms of the integration variables, are as follows:

$$\bar{\alpha} = \frac{\int_{z=0;\alpha=0}^{z=H;\alpha=\alpha_{max}} A\alpha \, dz}{\int_{z=0}^{z=H} A \, dz} = \frac{V_{bubbles}}{V_{vessel}}. \tag{54}$$

So this model is represented by three explicit first-order differential equations. They are vapor balance, and the bubble and enclosed volume equations (i.e., Eqs. (51), (55) and (56)).

For non-constant cross-sectional area vessels, the cross-sectional area approaches zero at the top and bottom of the vessel. The numeric integration fails at these locations. This failure is not a problem for the calculation of the average void fraction. One can start the integration at a very small height (e.g., $z = 10^{-6}$) and end the integration very close to the total height (e.g., $z = 0.999H$). The bubbles not included in the first 0.0001% and last 0.1% will not affect the average void fraction.

3. Conclusions

Analytic results are given for constant cross-sectional area vessels (e.g., vertical cylinders) and the two drift-flux correlations. These results relate the dimensionless superficial vapor velocity (ψ or Ξ), average void fraction ($\bar{\alpha}$), and local void fraction at the top of the vessel (α_{max}). For the churn-turbulent drift-flux correlation, a closed-form explicit solution is presented. For the DIERS' viscous-bubbly drift-flux correlation, an implicit solution is given. Thus, the relationships needed for the coupling equation are available.

For horizontal cylinders and spheres, numeric integration is required. The equations are manipulated to obtain three first-order ordinary differential equations. The local void fraction at the top of the vessel α_{max} is shown both by reasoning about the model and numeric results to go to the asymptote value of $1/Co$ for all dimensionless superficial vapor velocity ψ values. If correct, this would bring into question the assumption of a continuous liquid phase with a void fraction of less than 40%. However, this asymptote value wrongly implies only vapor will come out of the vessel when Co equals one (again these drift-flux models do not consider a gas-continuous regime). This problem may be due to the drift-flux relationship assuming momentum effects are negligible with respect to buoyancy effects. This will not be the case for the converging cross-sectional area. *Therefore, this α_{max} result should not be used in the coupling equation.* Further experimental work in this area is warranted.

In summary, the theoretical basis of the DIERS' disengagement model has been discussed along with the deviation of the resulting equations. By understanding the model better the engineer will have a greater appreciation of the applicability of these models to their pressure relief system design. These models are among the best available and are conservative. Further experimental and modeling for non-constant

cross-sectional area systems (and high-viscosity systems) are under consideration in order to improve our understanding.

Nomenclature

A	cross-sectional area of the vessel, ft^2 or m^2
Co	distribution parameter
$Energy_{input}$	energy input to the differential slice, Btu/s or J/s
g	gravitational constant, ft/s^2 or m/s^2
H	height of tank, ft or m
H_{liq}	liquid level in tank, ft or m
j	volumetric flux, ft/s or m/s
j_g	vapor volumetric flux, ft/s or m/s
$j_{g\infty}$	superficial vapor velocity at the top of a cross-sectional area vessel (ft/s or m/s)
j_{gf}	drift flux, ft/s or m/s
L	length of the horizontal cylinder
M_{liquid}	mass of the liquid in the differential slice, lb or kg
q	heat generation rate per mass of liquid, Btu/s lb or J/s kg
Q_{vapor}	volume of vapor produced in the differential slice, ft^3/s or m^3/s
R	radius of the horizontal cylinder and the sphere
U_∞	bubble rise velocity$\left(= 1.53 \sqrt[4]{\frac{\sigma g(\rho_f - \rho_g)}{\rho^2_f}}\right.$ (for churn turbulent, Ref. [12]) and $\left(= 1.18 \sqrt[4]{\frac{\sigma g(\rho_f - \rho_g)}{\rho_f^2}}\right.$ (for bubbly, Refs. [12])$\left.\right)\left.\right)$, ft/s or m/s
V_{vessel}	volume of vessel, ft^3 or m^3
$V_{bubbles}$	volume of bubbles in the vessel, ft^3 or m^3
W_{vapor}	mass of vapor produced in the differential slice, lb or kg
x	an intermediate term in Ref. [4] analytical integration for the DIERS' viscous-bubbly case
y	an intermediate term in Ref. [4] analytical integration for the DIERS' viscous-bubbly case
z	height from bottom of vessel, ft or m
z^*	dimensionless vertical height based on total vessel height not liquid height (z/H)

Greek letters

α	void fraction (percentage vapor)
$\bar{\alpha}$	average void fraction
α_{max}	maximum void fraction which occurs at the top of the vessel
λ	latent heat of vaporization, Btu/lb or J/kg

Ξ = modified dimensionless superficial vapor velocity [15] $\left(= \frac{\rho_f}{\rho_g} \frac{q}{\lambda} \frac{H}{U_\infty} = \frac{\psi}{(1-\bar{\alpha})}\right)$

ρ_f liquid density, lb/ft^3 or kg/m^3

ρ_g vapor density, lb/ft^3 or kg/m^3

σ surface tension, dyn/cm or N/m

ψ dimensionless superficial vapor velocity $\left(= \frac{\rho_f}{\rho_g} \frac{q}{\lambda} \frac{H(1-\bar{\alpha})}{U_\infty}\right)$

Acknowledgements

This research was conducted while C.M. Sheppard was a Visiting Scientist at the Safety Technology Institute at Joint Research Centre in Ispra, Italy. This support by the European Commission (Directorate - General XII - Science Research and Development) is gratefully acknowledged. Input from H. Fisher and the reviewers was very helpful.

References

[1] H.G. Fisher, H.S. Forrest, S.S. Grossel, J.E. Huff, A.R. Muller, J.A. Noronha, D.A. Shaw and B.J. Tilley, Emergency Relief System Design using DIERS Technology – Design Institute for Emergency Relief Systems (DIERS) Project Manual, AIChE Publication, New York, 1992.
[2] H.G. Fisher, Plant/Oper. Progress, 10 (1991) 1.
[3] C.M. Sheppard, J. Loss Prevention, 6 (1993) 177.
[4] S.D. Morris, USA DIERS Users Group Meeting, San Francisco, CA, May 1994.
[5] M.A. Grolmes and H.G. Fisher, Vapor–liquid onset/disengagement for emergency relief discharge evaluation, AIChE Summer Meeting, Denver, CO, August 1994.
[6] Fauske and Associates, Inc., Technology Summary, Emergency Relief Systems for Runaway Chemical Reactions and Storage Vessels: A Summary of Multiphase Flow Methods, AIChE/DIERS Publications, New York, 1986.
[7] C.M. Sheppard, J. Loss Prevention, 7 (1994) 3.
[8] M.A. Grolmes and H.G. Fisher, Paper to be presented at the International Symposium on Runaway Reactions and Pressure Relief Design, Boston, MA, August 1995.
[9] C.M. Sheppard, Drift-flux correlation disengagement models, part IV – Vent stream void fraction prediction for non-constant cross-sectional area vessels also considering entrainment, in preparation.
[10] M. Epstein, H.K. Fauske and G.M. Hauser, J. Loss Prevention Process Ind., 2 (1989) 45.
[11] N. Zuber and J. Findley, Trans. ASME J. Heat Transfer Ser. C, 87 (1965) 453.
[12] G.B. Wallis, One Dimensional Two-Phase Flow, McGraw-Hill, New York, 1969.
[13] H.G. Fisher, personal communication, 31 March 1992.
[14] C.M. Sheppard, Drift-flux correlation disengagement models, Part III – Shape-based correlations for disengagement prediction via bubbly drift-flux correlation, in preparation.
[15] C.M. Sheppard, Plant/Oper. Prog., 11 (1992) 229.
[16] C.M. Sheppard, J. Hazard. Mater., 44 (1995) 127.
[17] S.D. Morris, α_{max} in vessel: Some comments and further developments, DIERS Fall 1992 meeting, Princeton, NJ, October 1992.
[18] K. Bell, S.D. Morris and R. Oster, J. Loss Prevention Process Ind., 6 (1993) 31.
[19] S.D. Morris, K. Bell and R. Oster, Chem. Eng. Process., 31 (1992) 297.